

Nature of the Metal–Ligand Bond in $M(\text{CO})_5\text{PX}_3$ Complexes ($M = \text{Cr}, \text{Mo}, \text{W}$; $X = \text{H}, \text{Me}, \text{F}, \text{Cl}$): Synthesis, Molecular Structure, and Quantum-Chemical Calculations

Gernot Frenking,^{*,†} Karin Wichmann,[†] Nikolaus Fröhlich,[†] Joseph Grobe,^{*,‡} Winfried Golla,[‡] Duc Le Van,[‡] Bernt Krebs,[‡] and Mechtild Läge[‡]

Fachbereich Chemie, Philipps-Universität Marburg, Hans-Meerwein-Strasse, 35039 Marburg, Germany, and the Institut für Anorganische und Analytische Chemie, Westfälische Wilhelms-Universität Münster, Wilhelm-Klemm-Strasse 8, 48149 Münster, Germany

Received April 19, 2002

The syntheses of the phosphane complexes $M(\text{CO})_5\text{PH}_3$ ($M = \text{Mo}, \text{W}$), $\text{W}(\text{CO})_5\text{PD}_3$, and $\text{W}(\text{CO})_5\text{PF}_3$ and the results of X-ray structure analyses of $\text{W}(\text{CO})_5\text{PH}_3$ and $\text{Mo}(\text{CO})_5\text{PCL}_3$ are reported. Quantum-chemical DFT calculations of the geometries and M – P bond dissociation energies of $M(\text{CO})_5\text{PX}_3$ ($M = \text{Cr}, \text{Mo}, \text{W}$; $X = \text{H}, \text{Me}, \text{F}, \text{Cl}$) have been carried out. There is no correlation between the bond lengths and bond dissociation energies of the M – P bonds. The PMe_3 ligand forms the strongest and the longest M – P bonds of the phosphane ligands. The analysis of M – PX_3 bonds shows that PCl_3 is a poorer σ donor and a stronger $\pi(\text{P})$ acceptor than the other phosphanes. The energy decomposition analysis indicates that the M – P bonds of the PH_3 and PMe_3 complexes have a higher electrostatic than covalent character. The electrostatic contribution is between 56 and 66% of the total attractive interactions. The orbital interactions in the M – PH_3 and M – PMe_3 bonds have more σ character (65–75%) than π character (25–35%). The M – P bonds of the halophosphane complexes $M(\text{CO})_5\text{PF}_3$ and $M(\text{CO})_5\text{PCL}_3$ are nearly half covalent and half electrostatic. The π bonding contributes ~50% to the total orbital interaction.

Introduction

Phosphanes PX_3 are, besides CO , the most ubiquitous ligands in transition-metal chemistry. Metal complexes with phosphane ligands are interesting not only for academic research. Numerous representatives have been used as powerful catalysts in homolytically catalyzed chemical reactions which are important for industrial purposes.¹ It is well-known that the chemical behavior of PX_3 complexes can be modulated by the choice of the atom or group X . To tune the properties of the compounds, it is helpful to understand the nature of the M – PX_3 interactions.

Phosphane complexes of the type $M(\text{CO})_5\text{PX}_3$ ($M = \text{Cr}, \text{Mo}, \text{W}$; $X = \text{H}, \text{Me}, \text{F}, \text{Cl}, \text{Br}$) are of considerable interest both in preparative coordination chemistry and in studies of transition-metal–phosphorus bonds of low-oxidation-state compounds. Thus, the tungsten complex $\text{W}(\text{CO})_5\text{PH}_3$ has been used for the synthesis of a series of primary and secondary phosphanes in the coordination sphere of tungsten.² On the other hand, the halogenophosphane complexes $M(\text{CO})_5\text{PX}_3$ ($X = \text{Cl}, \text{Br}$) are suitable precursors for the generation of cluster

compounds, as demonstrated by the work of Huttner et al.³

During the past few decades the nature of the metal–phosphorus bond has been the subject of several theoretical studies^{4–16} and was investigated by a variety of

(3) Lang, H.; Huttner, G.; Zsolnai, L.; Mohr, G.; Sigwarth, B.; Weber, U.; Orama, O.; Jibril, I. *J. Organomet. Chem.* **1986**, *304*, 157–179.

(4) Reviews: (a) Fantucci, P. *Comments Inorg. Chem.* **1992**, *13*, 241–260. (b) Dias, P. B.; Minas de Piedade, M. E.; Martinho Simoes, J. A. *Coord. Chem. Rev.* **1994**, *135/136*, 738–807. (c) Alyea, E. C.; Song, S. *Comments Inorg. Chem.* **1996**, *18*, 145–164. (d) Alyea, E. C.; Song, S. *Comments Inorg. Chem.* **1996**, *18*, 189–221.

(5) (a) Xiao, S.; Trogler, W. C.; Ellis, D. E.; Berkovich-Yellin, Z. *J. Am. Chem. Soc.* **1983**, *105*, 7033–7037. (b) Marynick, D. S. *J. Am. Chem. Soc.* **1984**, *106*, 4064–4065.

(6) (a) Braga, M. *Inorg. Chem.* **1985**, *24*, 2702–2706. (b) Braga, M. *Quim. Nova* **1988**, *11*, 71–75.

(7) Orpen, A. G.; Connelly, N. G. *J. Chem. Soc., Chem. Commun.* **1985**, 1310–1311.

(8) Pacchioni, G.; Bagus, P. S. *Inorg. Chem.* **1992**, *31*, 4391–4398. (9) Van Wüllen, C. *J. Comput. Chem.* **1997**, *18*, 1985–1992.

(10) Jacobsen, H.; Berke, H. *Chem. Eur. J.* **1997**, *3*, 881–886.

(11) Bowmaker, G. A.; Schmidbaur, H.; Krüger, S.; Rösch, N. *Inorg. Chem.* **1997**, *36*, 1754–1757.

(12) Kaupp, M. *Chem. Ber.* **1996**, *129*, 535–544.

(13) Gonzáles-Blanco, Ö.; Branchadell, V. *Organometallics* **1997**, *16*, 5556–5562.

(14) (a) Dapprich, S.; Frenking, G. *Organometallics* **1996**, *15*, 4547–4551. (b) Frenking, G.; Dapprich, S.; Meisterknecht, T.; Uddin, J. *NATO Sci. Ser. C* **2000**, *546*, 73–89.

(15) Ruiz-Morales, Y.; Ziegler, T. *J. Phys. Chem. A* **1998**, *102*, 3970–3976.

(16) (a) Fernandez, A. L.; Wilson, M. R.; Prock, A.; Giering, W. P. *Organometallics* **2001**, *20*, 3429–3435. (b) Golovin, M. N.; Rahman, M. M.; Belmonte, J. E.; Giering, W. P. *Organometallics* **1985**, *4*, 1981. (c) Rahman, M. M.; Liu, H. Y.; Prock, A.; Giering, W. P. *Organome-*

[†] Philipps-Universität Marburg.

[‡] Westfälische Wilhelms-Universität Münster.

(1) Cornils, B.; Herrmann, W. A., Eds. *Applied Homogeneous Catalysis with Organometallic Compounds*; VCH: Weinheim, Germany, 1996.

(2) Nief, N.; Mercier, F.; Mathey, F. *J. Organomet. Chem.* **1987**, *328*, 349–355.

experimental techniques.^{4,17–20} However, the results obtained so far have led to controversial discussions, in particular with respect to the role of M→P back-bonding and the possible bonding mechanisms as well as about the σ and π contributions to the bond. The interpretation of IR data of phosphane complexes by means of the Cotton–Kraihanzel force-field technique²¹ led to the following order of π -acceptance: $\text{PF}_3 > \text{PCl}_3 > \text{P(OR)}_3 > \text{PR}_3$.²² The strength of the M→PX₃ π -back-donation has also been estimated from NMR spectroscopic data. Wang et al. measured the oxygen-17 quadrupole constants of (CO)₅W–PR₃ complexes and came to the conclusion that PMe₃ is a stronger π -accepting ligand than NMe₃ but weaker than P(OMe)₃.¹⁹ Alyea and Song reported experimental ⁹⁵Mo, ³¹P, and ¹³C NMR chemical shifts of (CO)_nMo–(PR₃)_{6–n} ($n = 3–5$) complexes.²⁰ The interpretation of the results and a reexamination of the various parameters used to evaluate σ and π contributions to the M–P bond led them to suggest that PCl₃ should be a weak π -acceptor.^{4c,d} However, a recent theoretical study of ⁹⁵Mo and ³¹P NMR chemical shifts of (CO)₅MoPR₃ by Ruiz-Morales and Ziegler showed that PCl₃ is actually a very strong π -acceptor that is stronger than PF₃ and, particularly, PH₃ and PMe₃.¹⁵

To gain a better insight into the M–P bond description, further information resulting from advanced theoretical calculations and additional structural data are necessary. Of particularly great help would be the structure determination of the parent complexes M(CO)₅PH₃ (M = Cr, Mo, W), which have been known from the work of Fischer and co-workers²³ for about 30 years. Therefore, we have put considerable effort into the preparation of some representatives and into the isolation of suitable single crystals for X-ray diffraction studies. An X-ray structure analysis of Cr(CO)₅PH₃ has been reported before by Huttner.²⁴ However, because of structural disorder it was not possible to give reliable bond lengths and angles of the PH₃ ligand. Here we report the first X-ray structure analysis of a transition-metal phosphane complex with one PH₃ ligand, W(CO)₅PH₃, which gives experimental bond lengths and angles. We also carried out theoretical investigations of the structures and the bonding situation of M(CO)₅PX₃ (M = Cr (**1**), Mo (**2**), W (**3**); X = H (**a**), Me (**b**), F (**c**), Cl (**d**)).

The quantum-chemical calculations of the geometries and bond dissociation energies and the theoretical

analysis of the (CO)₅M–PX₃ bonding were carried out using gradient-corrected DFT methods. We analyzed the electronic structure and the energy of the M–P bonds. The changes in the σ and π charges were investigated by NBO²⁵ population analysis. The contributions of electrostatic and covalent attraction to the M–PR₃ bonding and the strength of the σ and π contributions to the orbital interactions have been determined by the ETS²⁶ energy partitioning analysis. The same methods have recently been used by us to analyze the bonding in carbonyl complexes,²⁷ group 13 diyl complexes,²⁸ and complexes with cyclic π ligands.²⁹ Details about the ETS analysis are given there and in the Experimental Section.

The experimental results obtained are based on a novel effective synthesis of the complexes M(CO)₅PH₃ (M = Mo (**2a**), W(**3a**)), W(CO)₅PD₃ (**3e**), and W(CO)₅PF₃ (**3c**) as well as on X-ray diffraction analyses of **3a** and Mo(CO)₅PCL₃ (**2d**). As the latter complex was described in the literature^{3,18c} to be unstable, no structural data are known so far.

We wish to comment on the way the topic of π -acceptor strength of ligands is frequently addressed and discussed in the literature. Many workers take the correlation between a measured quantity, such as a vibrational frequency or a force constant, NMR chemical shift components, or coupling constants, and selected theoretical data such as orbital populations as a measure of π -acceptor strength. While such procedures may be helpful to establish an ordering scheme of the ligands, they can be deceptive, because any observable quantity is the result of the *total* interactions between the ligand and the complex fragment. Without an explicit analysis of the actual changes of the σ and π charges and the associated effects on the observed properties, any statement about π -acceptor strength remains a speculation. For example, the QALE (quantitative analysis of ligand effects)¹⁶ method has been developed as a mathematical tool to correlate the properties of phosphane ligands with so-called stereo-electronic parameters, which are then suggested as an indicator of π -acceptor strength. It is questionable whether a good correlation between different parameters is indicative of a real physical change in the electronic structure. We also want to point out that the relative π -acceptor strength of ligands can only be established with respect to a given complex fragment. Two ligands may have a reverse π -acceptor strength in combination with complex fragments of two different metals. Therefore, a description of the π -acceptor strength of ligands without a metal donor fragment as reference seems questionable. Finally, we want to mention that π -acceptor interactions may have different effects on experimental parameters. Vibrational spectra, NMR chemical shifts or coupling constants, and bond energies are affected to a different extent by π -acceptor interac-

tallics **1987**, *6*, 650. (d) Rahman, M. M.; Liu, H. Y.; Eriks, K.; Prock, A.; Giering, W. P. *Organometallics* **1989**, *8*, 1. (e) Liu, H. Y.; Eriks, K.; Giering, W. P.; Prock, A. *Inorg. Chem.* **1989**, *28*, 1759. (f) Liu, H. Y.; Eriks, K.; Prock, A.; Giering, W. P. *Organometallics* **1990**, *9*, 1758. (g) Wilson, M. R.; Woska, D. C.; Prock, A. *Organometallics* **1993**, *12*, 1742.

(17) (a) Graham, W. A. G. *Inorg. Chem.* **1968**, *7*, 315–321. (b) Nolan, S. P.; Hoff, C. D. *J. Organomet. Chem.* **1985**, *290*, 365–373.

(18) (a) Davies, M. S.; Pierens, R. K.; Aroney, M. J. *J. Organomet. Chem.* **1993**, *458*, 141–146. (b) Aroney, M. J.; Buys, I. E.; Davies, M. S.; Hambley, T. W. *J. Chem. Soc., Dalton Trans.* **1994**, 2827–2834. (c) Davies, M. S.; Aroney, M. J.; Buys, I. E.; Hambley, T. W.; Calvert, J. L. *Inorg. Chem.* **1995**, *34*, 330–336.

(19) Wang, S. P.; Richmond, M. G.; Schwartz, M. *J. Am. Chem. Soc.* **1992**, *114*, 7595–7596.

(20) Alyea, E. C.; Song, S. *Inorg. Chem.* **1995**, *34*, 3864–3873.

(21) Cotton, F. A.; Kraihanzel, C. S. *J. Am. Chem. Soc.* **1962**, *84*, 4432–4438.

(22) Huheey, J. E.; Keiter, E. A.; Keiter, R. L. *Inorganic Chemistry: Principles and Structure of Reactivity*, 4th ed.; Harper Collins College: New York, 1993; p 431.

(23) Fischer, E. O.; Louis, E.; Bathelt, W.; Müller, J. *Chem. Ber.* **1969**, *102*, 2547–2556.

(24) Huttner, G.; Schelle, S. *J. Organomet. Chem.* **1973**, *47*, 383–390.

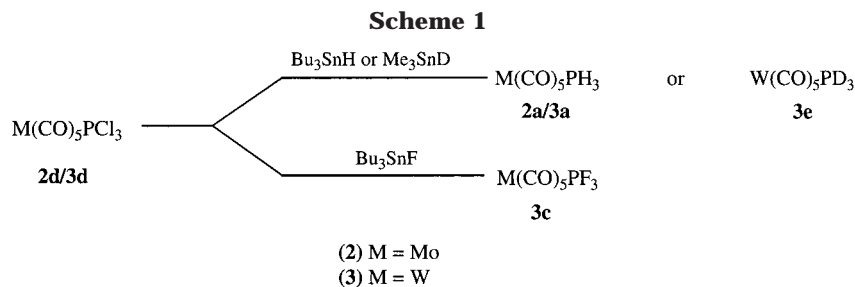
(25) Reed, A. E.; Weinhold, F.; Curtiss, F. *Chem. Rev.* **1985**, *88*, 899.

(26) (a) Ziegler, T.; Rauk, A. *Theor. Chim. Acta* **1977**, *46*, 1. (b) Ziegler, T.; Rauk, A. *Inorg. Chem.* **1979**, *18*, 1558. (c) Ziegler, T.; Rauk, A. *Inorg. Chem.* **1979**, *18*, 1755.

(27) Diefenbach, A.; Bickelhaupt, F. M.; Frenking, G. *J. Am. Chem. Soc.* **2000**, *122*, 6449–6458.

(28) (a) Uddin, J.; Frenking, G. *J. Am. Chem. Soc.* **2001**, *123*, 1683–1693. (b) Chen, Y.; Frenking, G. *J. Chem. Soc., Dalton Trans.* **2001**, 434–440.

(29) Lein, M.; Frunzke, J.; Timoshkin, A. *Chem. Eur. J.* **2001**, *7*, 4155–4163.



tions. Consequently, statements about the alleged strength or weakness of a ligand as a π -acceptor should be made with caution.

Experimental Section

Syntheses. The phosphane complexes $M(\text{CO})_5\text{PH}_3$ and $M(\text{CO})_5\text{PF}_3$ ($M = \text{Cr}, \text{Mo}, \text{W}$) have been prepared earlier either by photochemical^{23,30} or by thermal³¹ substitution from the metal hexacarbonyls and the ligands as precursors. As a rule, labile compounds such as $M(\text{CO})_5(\text{THF})$ and $M(\text{CO})_5(\text{CH}_2\text{Cl}_2)$ were used as intermediates. However, the yields obtained were very low: e.g., only 2% for the complexes $M(\text{CO})_5\text{PH}_3$.²³ This is partly due to the fact that the highly toxic, gaseous, and spontaneously inflammable ligand PH_3 is difficult to handle in preparative amounts. A more suitable synthesis of the tungsten complex was developed by Mathey et al.² by the reaction of $\text{W}(\text{CO})_5(\text{THF})$ or $\text{W}(\text{CO})_5(\text{CH}_3\text{CN})$ with phosphonium iodide, PH_4I .

In our preparation the chlorophosphane complexes $M(\text{CO})_5\text{PCL}_3$ ($M = \text{Mo}$ (**2d**), W (**3d**)) were employed as precursors for the corresponding PH_3 or PF_3 derivatives. Compounds **2d** and **3d** were produced by the "indirect" photochemical method³² via the labile intermediate $M(\text{CO})_5(\text{THF})$. As shown in Scheme 1, the chlorine substituents of the coordinated PCL_3 can be replaced by hydrogen or fluorine using organotin hydrides R_3SnH or fluorides R_3SnF as reagents.

With the exception of compound **2a** the complexes **2** and **3** are obtained in high purity and almost quantitative yields. Because the reaction of **2d** with Bu_3SnH is much slower than that of **3d** (4 days vs 2 h) under comparable conditions, a gradual decomposition of **2a** is observed in the reaction mixture, leading to a lower isolated yield.

The composition and constitution of the complexes **2** and **3** were investigated by MS, IR, and NMR (^1H , ^{13}C , ^{31}P , ^{19}F (**3c**)) spectroscopy and compared with the literature data. X-ray diffraction analyses were carried out on single crystals of **2d** and **3a**.

General Techniques. All experiments were performed using standard vacuum line techniques or Schlenk methods under an argon atmosphere. Reaction vessels were either Schlenk flasks or ampules with several break-seals and a side-attached NMR tube. Solvents and deuterated compounds for NMR measurements were carefully dried and degassed. NMR: Bruker AC 200 (200.13 MHz, ^1H , standard TMS; 50.32 MHz, ^{13}C , standard TMS; 81.02 MHz, ^{31}P , standard 85% H_3PO_4 ; 188.31 MHz, ^{19}F , standard CCl_3F). MS: Model MAT 212, Varian MAT. IR: Nicolet Impact 400, Bruker IFS 48.

(Phosphane)pentacarbonylmolybdenum (2a). A 224 mg (0.60 mmol) portion of $\text{Mo}(\text{CO})_5\text{PCL}_3$ (**2d**) was dissolved in a Schlenk vessel in 1 mL of pentane. After dropwise addition of a solution of 523 mg (1.80 mmol) of Bu_3SnH in 1 mL of pentane at room temperature, the mixture was stirred in the dark. The course of the reaction was followed by ^{31}P NMR measurements. The replacement of Cl by H was found to be

complete after 4 days. **2a** was obtained as colorless crystals and purified by washing the filter residue with cold pentane (0 °C). The complex was characterized by comparing the spectroscopic parameters with literature data.²³ Yield: 79 mg (0.29 mmol), 49%.

(Phosphane)pentacarbonyltungsten (3a). The synthesis was analogous to that of **2a**: 407 mg (0.88 mmol) of $\text{W}(\text{CO})_5\text{PCL}_3$ (**3d**), 808 mg (2.78 mmol) of Bu_3SnH ; reaction time 2 h. Yield: 287 mg (0.80 mmol), 91%. Characterization was achieved by comparison of the various spectra with literature data.²³ Additional information: ^{13}C NMR (C_6D_6 , 25 °C) δ 195.1 (d, $^2J(\text{P},\text{C}) = 7.2$ Hz, cis CO), 197.9 (d, $^2J(\text{P},\text{C}) = 11.7$ Hz, trans CO).

(d₃-Phosphane)pentacarbonyltungsten (3e). The synthesis was analogous to that of **2a**: 123 mg (0.27 mmol) of $\text{W}(\text{CO})_5\text{PCL}_3$ (**3d**), 150 mg (0.91 mmol) of Me_3SnD ; solvent, 0.5 mL of pentane; reaction vessel, NMR tube; reaction time, 3 h. Yield: 96 mg (0.27 mmol), 99%. ^{31}P NMR (C_6D_6 , 25 °C): δ -185.9 (tt with ^{183}W satellites, $^1J(\text{P},\text{D}) = 52.3$ Hz, $^1J(\text{W},\text{P}) = 215.2$ Hz).

(Trifluorophosphane)pentacarbonyltungsten (3c). To a suspension of 316 mg (1.02 mmol) of Bu_3SnF in 1 mL of pentane placed in a Schlenk vessel was added a solution of 155 mg (0.34 mmol) of $\text{W}(\text{CO})_5\text{PCL}_3$ (**3d**) in 1 mL of pentane. The mixture was stirred in the dark for 2 days. Only a trace of Bu_3SnF remained unreacted after this time. The solvent was pumped off in vacuo at -78 °C, and the volatile complex $\text{W}(\text{CO})_5\text{PF}_3$ was then condensed from the reaction vessel (kept at -18 °C) into a -196 °C trap. Yield: 131 mg (0.32 mmol), 95%. The product was characterized by comparing the various spectra with literature data (IR,³⁰ NMR^{33,34} incomplete). ^{31}P NMR (C_6D_6 , 25 °C): δ 120.6 (q with ^{183}W satellites, $^1J(\text{P},\text{F}) = 1288.5$ Hz, $^1J(\text{W},\text{P}) = 496.3$ Hz). ^{19}F NMR (C_6D_6 , 25 °C): δ -7.6 (q with ^{183}W satellites, $^1J(\text{P},\text{F}) = 1288.8$ Hz, $^2J(\text{W},\text{F}) = 30.5$ Hz). MS (EI, 70 eV, selected, relative to ^{184}W): m/z (%) 412 (61) [M^+], 384 (5) [$\text{M}^+ - \text{CO}$], 356 (17) [$\text{M}^+ - 2 \text{CO}$], 328 (24) [$\text{M}^+ - 3 \text{CO}$], 324 (7) [$\text{M}^+ - \text{PF}_3$], 300 (10) [$\text{M}^+ - 4 \text{CO}$], 268 (100) [$\text{M}^+ - 2 \text{CO} - \text{PF}_3$].

X-ray Structural Analyses of 2d and 3a. Single crystals of good quality were obtained by crystallization from pentane solution. Crystal data and details of the data collection and structure solution for **2d** and **3a** are summarized in Table 1.

Quantum-Chemical Calculations. The calculations were performed at the nonlocal DFT level of theory using the exchange functional of Becke³⁵ and the correlation functional of Perdew³⁶ (BP86). Scalar relativistic effects have been considered using the zero-order regular approximation (ZO-RA).³⁷ Uncontracted Slater-type orbitals (STOs) were used as basis functions for the SCF calculations.³⁸ The basis sets for the metal atoms have triple- ζ quality augmented with one (n)p function. Triple- ζ basis sets augmented by two sets of polariza-

(33) Keiter, R. L.; Verkade, J. G. *Inorg. Chem.* **1969**, *8*, 2115–2120.

(34) Mercier, F.; Mathey, F.; Afiong-Akpan, C.; Nixon, J. F. *J. Organomet. Chem.* **1988**, *348*, 361–367.

(35) Becke, A. D. *Phys. Rev. A* **1988**, *38*, 3098.

(36) Perdew, J. P. *Phys. Rev. B* **1986**, *33*, 8822.

(37) (a) Snijders, J. G. *Mol. Phys.* **1978**, *36*, 1789. (b) Snijders, J. G.; Ross, P. *Mol. Phys.* **1979**, *38*, 1909.

(38) Snijders, J. G.; Baerends, E. J.; Vernooijs, P. *At. Nucl. Data Tables* **1982**, *26*, 483.

(30) Strauss, S. H.; Abrey, K. D. *Inorg. Chem.* **1984**, *23*, 516–518.

(31) Ogilvie, F.; Clark, R. J.; Verkade, J. G. *Inorg. Chem.* **1969**, *8*, 1904–1907.

(32) Strohmeier, W.; Müller, F. J. *Chem. Ber.* **1969**, *102*, 3608–3615.

Table 1. Crystallographic Data and Parameters of the Crystal Structure Determinations

	2d	3a
empirical formula	C ₅ MoO ₅ PCl ₃	C ₅ H ₃ O ₅ PW
fw	373.31	357.90
cryst size (mm)	0.15 × 0.12 × 0.09	0.20 × 0.12 × 0.02
cryst syst	monoclinic	monoclinic
space group	<i>P</i> 2 ₁ / <i>c</i>	<i>P</i> 2 ₁ / <i>c</i>
<i>a</i> (Å)	6.805(2)	10.864(3)
<i>b</i> (Å)	13.091(3)	6.689(2)
<i>c</i> (Å)	13.044(3)	12.537(4)
β (deg)	91.52	97.17
<i>V</i> (Å ³)	1161.6(5)	903.9(5)
<i>Z</i>	4	4
ρ _{calcd} (g cm ⁻³)	2.135	2.630
μ (mm ⁻¹)	1.950	12.935
<i>F</i> (000)	712	648
temperature (K)	150	173
2θ _{max} (deg)	54.11	54.11
index ranges	-6 ≤ <i>h</i> ≤ 8 -4 ≤ <i>k</i> ≤ 16 -16 ≤ <i>l</i> ≤ 16	0 ≤ <i>h</i> ≤ 13 0 ≤ <i>k</i> ≤ 8 -16 ≤ <i>l</i> ≤ 16
no. of rflns measd	2538	2047
no. of indep rflns with <i>I</i> > 2σ(<i>I</i>)	2262	1956
no. of params	137	109
R1	0.0189	0.0443
wR2	0.0450	0.1250
GOF on <i>F</i> ²	1.030	1.043
resid electron density (e Å ⁻³)	+0.657/-0.291	+3.322/-3.453

tion functions were used for the other atoms: i.e., 2p and 3d on hydrogen and 3d and 4f on the remaining main-group elements. This basis set combination is denoted as basis I. The $(n-1)s^2$ and $(n-1)p^6$ core electrons of the main-group elements and the $(n-1)s^2$, $(n-1)p^6$, $(n-1)d^{10}$, and $(n-1)f^{14}$ core electrons of the transition metals were treated by the frozen-core approximation.³⁹ An auxiliary set of s, p, d, f, and g STOs was used to fit the molecular densities and to represent the Coulomb and exchange potentials accurately in each SCF cycle.⁴⁰ The calculations were carried out with the program packages ADF99 and ADF2.3.⁴¹ To find out if the optimized structures are minima on the potential energy surface, we calculated the vibrational frequencies of the stationary points. The frequency calculations were carried out at BP86 with our standard basis set II⁴² using BP86/II optimized geometries, which were found to be very similar to the BP86/I data.⁴³ This was done with the program package Gaussian 98,⁴⁴ which has

(39) Baerends, E. J.; Ellis, D. E.; Ros, P. *Chem. Phys.* **1973**, *2*, 41.

(40) Krijn, J.; Baerends, E. J. Fit Functions in the HFS-Method, Internal Report (in Dutch); Vrije Universiteit Amsterdam, Amsterdam, The Netherlands, 1984.

(41) (a) Bickelhaupt, F. M.; Baerends, E. J. *Rev. Comput. Chem.* **2000**, *15*, 1–86. (b) te Velde, G.; Bickelhaupt, F. M.; Baerends, E. J.; van Gisbergen, S. J. A.; Fonseca Guerra, C.; Snijders, J. G.; Ziegler, T. *J. Comput. Chem.* **2001**, *22*, 931–967.

(42) Frenking, G.; Antes, I.; Böhme, M.; Dapprich, S.; Ehlers, A. W.; Jonas, V.; Neuhaus, A.; Otto, M.; Stegmann, R.; Veldkamp, A.; Vydroshchikov, S. F. In *Reviews in Computational Chemistry*; Lipkowitz, K. B., Boyd, D. B., Eds.; VCH: New York, 1996; Vol. 8, pp 63–144.

(43) Wichmann, K. Diplom Thesis, Philipps-Universität Marburg, 1999.

(44) Frisch, M. J.; Trucks, G. W.; Schlegel, H. B.; Scuseria, G. E.; Robb, M. A.; Cheeseman, J. R.; Zakrzewski, V. G.; Montgomery, J. A., Jr.; Stratmann, R. E.; Burant, J. C.; Dapprich, S.; Millam, J. M.; Daniels, A. D.; Kudin, K. N.; Strain, M. C.; Farkas, O.; Tomasi, J.; Barone, V.; Cossi, M.; Cammi, R.; Mennucci, B.; Pomelli, C.; Adamo, C.; Clifford, S.; Ochterski, J.; Petersson, G. A.; Ayala, P. Y.; Cui, Q.; Morokuma, K.; Malick, D. K.; Rabuck, A. D.; Raghavachari, K.; Foresman, J. B.; Cioslowski, J.; Ortiz, J. V.; Stefanov, B. B.; Liu, G.; Liashenko, A.; Piskorz, P.; Komaromi, I.; Gomperts, R.; Martin, R. L.; Fox, D. J.; Keith, T.; Al-Laham, M. A.; Peng, C. Y.; Nanayakkara, A.; Gonzalez, C.; Challacombe, M.; Gill, P. M. W.; Johnson, B. G.; Chen, W.; Wong, M. W.; Andres, J. L.; Head-Gordon, M.; Replogle, E. S.; Pople, J. A. *Gaussian 98*, revision A.3; Gaussian, Inc.: Pittsburgh, PA, 1998.

analytical second derivatives. For some molecules we carried out frequency calculations at BP86/I using numerical second derivatives. The molecular geometries were optimized with *C_s* symmetry constraint. This was done in order to obtain molecular orbitals with *a'* and *a''* symmetry for the subsequent energy analysis. We optimized the (CO)₅M–PX₃ structures with conformations where the PX₃ group is either staggered or eclipsed with respect to the cis-CO ligands. In all cases the energies of the two conformations were very similar, with differences < 1 kcal mol⁻¹. The frequency analyses showed that some complexes had staggered energy minima, some had eclipsed minima, and some structures did not have minima with *C_s* symmetry. Because the bond lengths and bond angles of the two conformations were nearly identical, in all cases the structures with staggered conformations were used for the bonding analysis.

The bonding interactions between the complex fragment M(CO)₅ and the ligands PX₃ have been analyzed with the energy decomposition scheme ETS developed by Ziegler and Rauk.²⁶ The bond dissociation energy Δ*E* between two fragments A and B (in the present case M(CO)₅ and PX₃) is partitioned into several contributions which can be identified as physically meaningful entities. First, Δ*E* is separated into two major components Δ*E*_{prep} and Δ*E*_{int}:

$$\Delta E = \Delta E_{\text{prep}} + \Delta E_{\text{int}} \quad (1)$$

Δ*E*_{prep} is the energy necessary to promote the fragments A and B from their equilibrium geometry and electronic ground state to the geometry and electronic state in the compound AB. Δ*E*_{int} is the instantaneous interaction energy between the two fragments in the molecule. The latter quantity will be the focus of the present work. The interaction energy Δ*E*_{int} can be divided into three main components:

$$\Delta E_{\text{int}} = \Delta E_{\text{elstat}} + \Delta E_{\text{Pauli}} + \Delta E_{\text{orb}} \quad (2)$$

Δ*E*_{elstat} gives the electrostatic interaction energies between the fragments, which are calculated with the frozen electron density distribution of A and B in the geometry of the complex AB. The second term in eq 2, Δ*E*_{Pauli}, gives the repulsive interactions between the fragments, which are caused by the fact that two electrons with the same spin cannot occupy the same region in space. The term comprises the four-electron destabilizing interactions between occupied orbitals. Δ*E*_{Pauli} is calculated by enforcing the Kohn–Sham determinant of AB, which results from superimposing fragments A and B, to obey the Pauli principle by antisymmetrization and renormalization. The stabilizing orbital interaction term Δ*E*_{orb} is calculated in the final step of the ETS analysis, when the Kohn–Sham orbitals relax to their optimal form. The latter term can be further partitioned into contributions by the orbitals which belong to different irreducible representations of the interacting system.

Unfortunately, the first two terms Δ*E*_{elstat} and Δ*E*_{Pauli} are often added up as the single term Δ*E*^σ, which is sometimes called the “steric energy term”.⁴⁵ Δ*E*^σ has nothing to do with the loosely defined steric interaction which is often used to explain the repulsive interactions of bulky substituents. Since Δ*E*_{elstat} is usually attractive and Δ*E*_{Pauli} repulsive, the two terms may largely cancel each other, and the focus of the discussion of the bonding interactions then rests on the orbital interaction term Δ*E*_{orb}. This leads to the deceptive description of the bonding only in terms of orbital interactions. The important information about the electrostatic/covalent character of the bond given by the ratio Δ*E*_{elstat}/Δ*E*_{orb} is then lost.

(45) Examples: (a) Ziegler, T.; Tschinke, V.; Becke, A. *J. Am. Chem. Soc.* **1987**, *109*, 1351. (b) Ziegler, T.; Tschinke, V.; Ursenbach, C. *J. Am. Chem. Soc.* **1987**, *109*, 4825. (c) Li, J.; Schreckenbach, G.; Ziegler, T. *J. Am. Chem. Soc.* **1995**, *117*, 486.

Geometries and Bond Dissociation Energies

Figure 1 shows the optimized structures of the phosphane complexes together with the theoretically predicted and experimentally observed bond lengths and angles. We will first discuss the geometries of $\text{Mo}(\text{CO})_5\text{PCl}_3$ (**2d**) and $\text{W}(\text{CO})_5\text{PH}_3$ (**3a**). The full set of calculated and experimental bond lengths and bond angles and the atomic coordinates and equivalent isotropic displacement parameters obtained from the X-ray structure analyses are given as Supporting Information.

Experiment and theory agree that the $\text{M}(\text{CO})_5$ moieties of **2d** and **3a** have a nearly perfect square-pyramidal geometry. The bond angles between the CO groups are always close to 90° . There is no tilting of the cis CO groups toward trans CO or toward the PX_3 ligand. The experimental and theoretical values show that the PCl_3 group of **2d** has nearly C_{3v} symmetry. The same is true for the theoretical structure of the PH_3 ligand in **3a**. The agreement between the calculated and experimental bond lengths and angles of **2d** and **3a** is quite good. The largest difference is found between the theoretical and experimental Mo–P distance of **2d**. The calculated value (2.467 Å) is clearly larger than the experimental number (2.379 Å). The difference is at least partly due to crystal packing effects. We have shown in systematic studies of donor/acceptor complexes of transition metals^{46a} and main-group elements^{46b} that the interatomic distances between the donor and the acceptor atom are *always* shorter in the solid state than in the gas phase. There is a correlation between the intrinsic bond dissociation energy (BDE) and the bond shortening of the donor/acceptor bond: i.e., the bond shortening tends to become larger if the bond is weaker. The largest difference of a donor/acceptor bond length between the solid state and the gas phase was ~ 1 Å.^{46b} Figure 1 shows that the calculated value of the W–P bond of **3a** (2.524 Å) is also longer than the experimental value (2.493 Å), but the difference is less than in the case of **2d**. The BDE of the Mo–P bond of **2d** ($D_e = 23.7$ kcal mol⁻¹) is less than the BDE of the W–P bond of **3a** ($D_e = 34.0$ kcal mol⁻¹), which is in agreement with the aforementioned correlation. We do not conclude that there is a quantitative correlation between bond energy and bond shortening between the gas-phase and solid-state structure of a donor/acceptor complex. We do want to point out, however, that the calculated M– PX_3 bond lengths shown in Figure 1 are *always* larger than the experimental values. Part of the difference is due to crystal-packing effects, and part may be due to the error of the theoretical method, giving atomic distances that are slightly too long.

The calculated and experimental metal–CO distances show that the CO ligands cis to the PX_3 group always have longer bonds than the trans-CO group. Note that the PF_3 and PCl_3 complexes which always have the shortest (but *not* the strongest; see below) M–P bonds of the PX_3 complexes (Figure 1) also contain the longest M–CO(trans) bonds. This result supports the model of competitive M→L back-bonding for ligands which are trans to each other.

(46) (a) Diedenhofen, M.; Wagener, T.; Frenking, G. In *Computational Organometallic Chemistry*; Cundari, T. R., Ed.; Marcel Dekker: New York, 2001; pp 69–121. (b) Jonas, V.; Frenking, G.; Reetz, M. T. *J. Am. Chem. Soc.* **1994**, *116*, 8741.

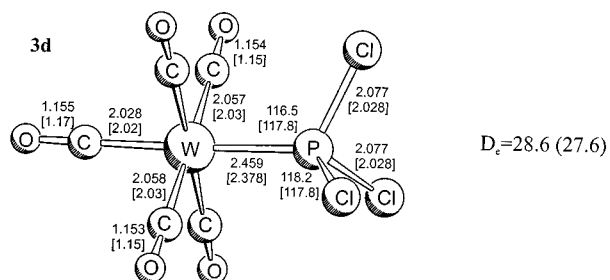
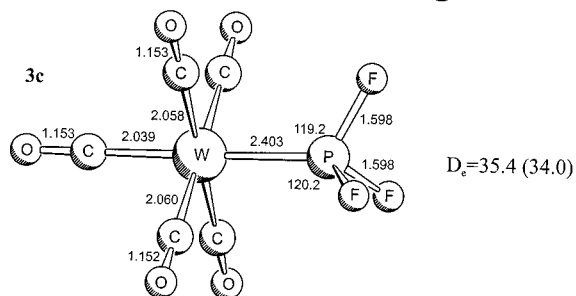
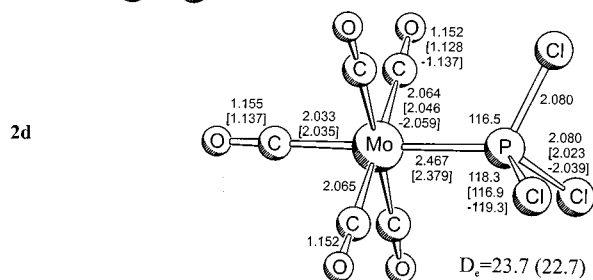
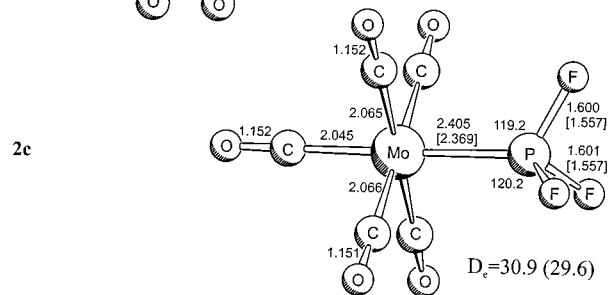
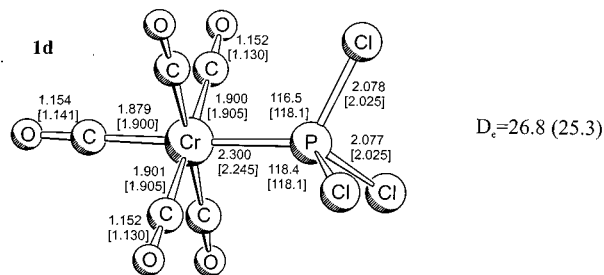
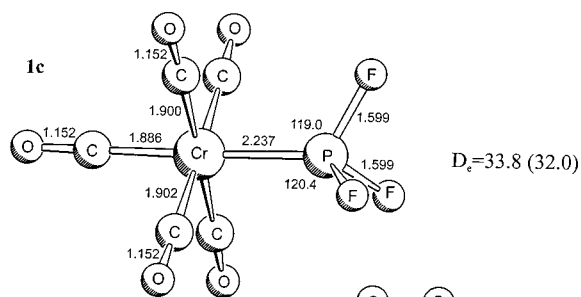
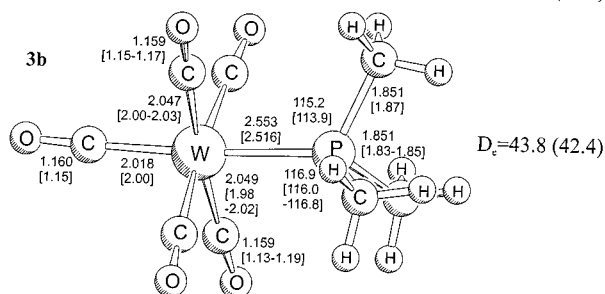
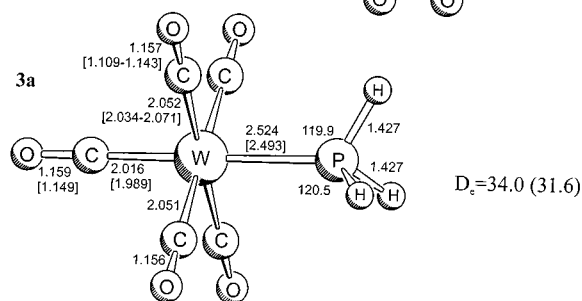
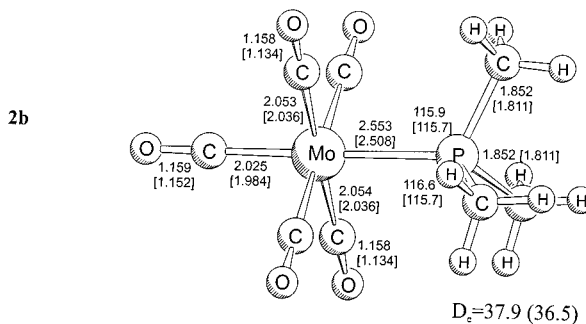
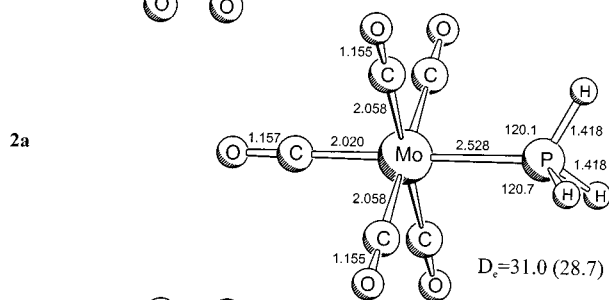
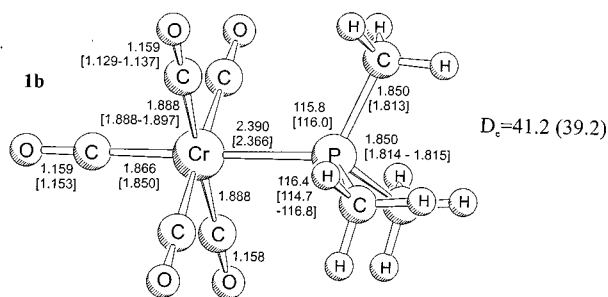
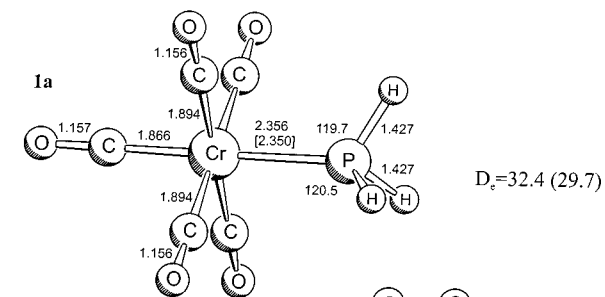
Figure 1 also gives the calculated and experimental geometries of the free ligands PX_3 and the theoretical geometries of the complex fragments $\text{M}(\text{CO})_5$. The theoretical and experimental bond lengths and angles of PX_3 are in good to reasonable agreement. The calculated bond lengths are always larger than the experimental values, particularly for the phosphorus–halogen bonds. The comparison of the fragment geometries with the bond lengths and angles of the complexes gives interesting information about the changes which are induced by M– PX_3 bond formation. The axial M–CO bonds of $\text{M}(\text{CO})_5$ trans to the hole are significantly shorter than the equatorial bonds. They become clearly longer in $(\text{CO})_5\text{MPX}_3$ but remain shorter than the cis M–CO bonds. Note that the P–X bonds of the PX_3 ligands in the complexes are always ~ 0.01 – 0.02 Å shorter than in free PX_3 . This could be taken as an argument that the M→ PX_3 π -back-donation takes place into the empty $d(\pi)$ orbital of phosphorus rather than into the P–X σ^* -antibonding orbitals as generally assumed,^{6a,47} because donation into the latter orbitals should yield longer P–X bonds. We do not think that this is a valid argument, because two other effects may be responsible for the P–X bond shortening. One is the change in hybridization of the P–X bonds. It will be shown below that the phosphorus lone-pair orbital in the free ligand has a large percentage of s character. Upon formation of the M–P bond the lone-pair phosphorus donor orbital achieves mainly p character, while the hybridization of the P–X bonds at phosphorus changes toward larger percent s character. According to Bent's rule,⁴⁸ this leads to shorter P–X bonds. The second effect comes from the change of the atomic partial charge of the phosphorus atoms in the complexes, which become more positively charged because of P→M charge donation. The higher positive charge at the P atom induces X→P charge donation, which may also lead to shorter P–X bonds in the complexes.

Figure 1 also presents the theoretically predicted M– PX_3 bond energies. The only experimental values which are available for comparison have been reported by Nolan and Hoff.^{17b} These workers measured the heats of reaction of phosphines and phosphites with the (toluene) $\text{Mo}(\text{CO})_3$ complex. They estimated the average molybdenum–phosphane bond strength in $(\text{CO})_3\text{Mo}(\text{PR}_3)_3$ complexes as Mo– $\text{PMe}_3 = 38.4$ kcal mol⁻¹ and Mo– $\text{PCl}_3 = 30.2$ kcal mol⁻¹. Our calculated values for $(\text{CO})_5\text{Mo}(\text{PMe}_3)$ ($D_0 = 36.5$ kcal mol⁻¹) and $(\text{CO})_5\text{Mo}(\text{PCl}_3)$ ($D_0 = 22.7$ kcal mol⁻¹) are in good to fair agreement with the experimental data.

Previous calculations of the complexes with PH_3 and PMe_3 ligands by van Wüllen⁹ gave results very similar to those in our work. The data for $(\text{CO})_5\text{M}(\text{PF}_3)$ and $(\text{CO})_5\text{M}(\text{PCl}_3)$ are, to the best of our knowledge, the first reliable bond energies published so far. The calculations show clearly that there is no correlation between bond lengths and bond energies. The most strongly bonded ligand, PMe_3 , has always the longest M– PX_3 bonds. The long M– PMe_3 bonds are not caused by steric repulsion

(47) (a) Xiao, S.-X.; Trogler, W. C.; Ellis, D. E.; Berkovich-Yellin, Z. *J. Am. Chem. Soc.* **1983**, *105*, 7033. (b) Marynick, D. S. *J. Am. Chem. Soc.* **1984**, *106*, 4064. (c) Orpen, A. G.; Connolly, N. G. *J. Chem. Soc., Chem. Commun.* **1985**, 1310.

(48) (a) Bent, H. A. *Chem. Rev.* **1961**, *61*, 275. (b) Jonas, V.; Boehme, C.; Frenking, G. *Inorg. Chem.* **1996**, 2097.



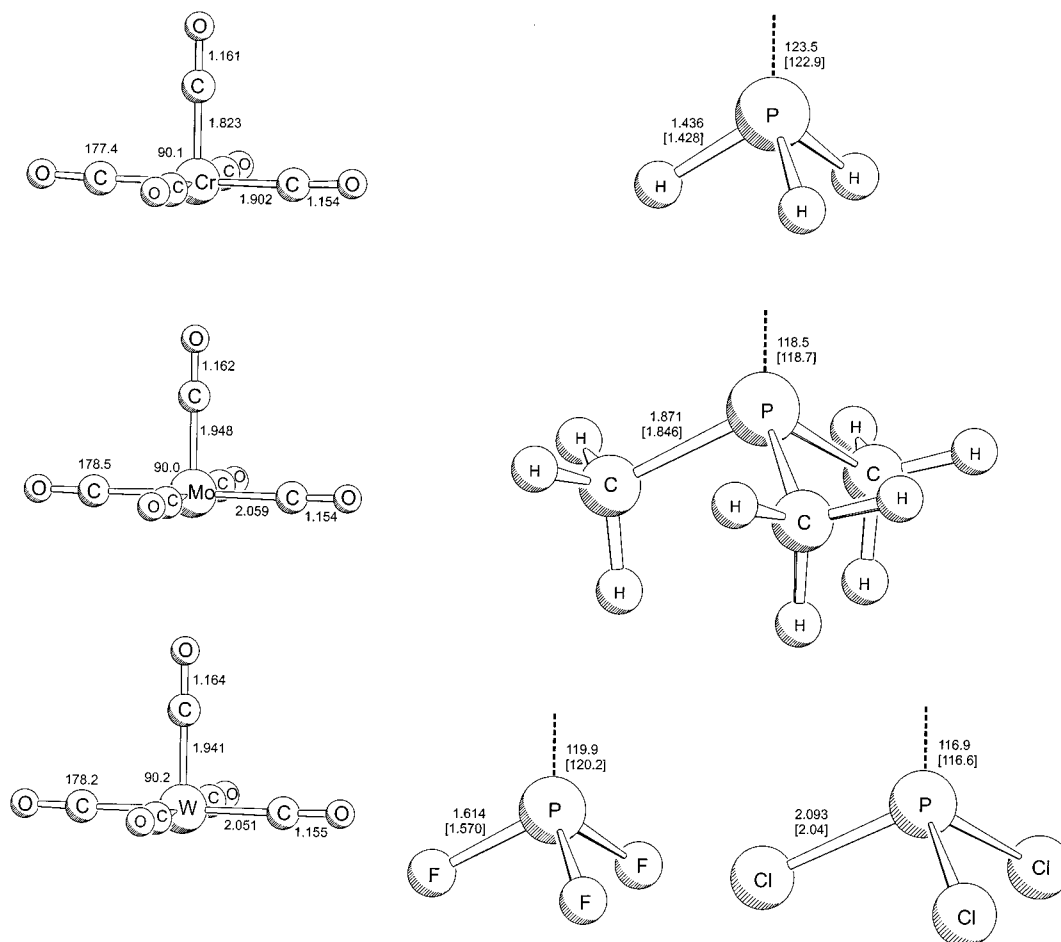


Figure 1. Geometries of the phosphane complexes $M(\text{CO})_5\text{PX}_3$ (**1a–d**, **2a–d**, **3a–d**, and **4a–d**). The most important calculated bond lengths (Å) and angles (deg) are shown. Experimental values are given in parentheses. The M–P bond length of **1a** is the average value of the two positions of the phosphorus atom in the disordered structures (2.351 and 2.347 Å) which have been reported in ref 24. The experimental values of **3a** and **2d** are from this work. The full set of data is given in Tables S1 and S2 of the Supporting Information. The other experimental values have been taken from refs 52 (**1b**), 18c (**2b**, **1d**, **3d**), 53 (**3b**), 54 (**2c**), 55 (PH_3), 56 (PMe_3), 57 (PF_3), and 58 (PCl_3).

between the methyl substituents and the cis-CO ligands. This becomes evident by comparing the bond angles M–P–X for X = Me, H, which are *smaller* for Me than for H (Figure 1). The BDEs of the phosphane ligands show for all metals the trend $\text{PMe}_3 > \text{PF}_3 \approx \text{PH}_3 > \text{PCl}_3$, while the calculated M– PX_3 interatomic distances decrease in the series $\text{PMe}_3 > \text{PH}_3 > \text{PCl}_3 > \text{PF}_3$. It has been noted before that metal–ligand bond lengths of donor/acceptor complexes are not reliable indicators of the bond strength.^{11,49,50} The finding that longer bonds may be stronger than shorter ones has been explained by the hybridization of the σ -donor orbital.⁵⁰ A higher percent s character leads to more compact orbitals and thus results in shorter interatomic distances. A higher percent s character of the donor orbitals at the same time yields weaker donor/acceptor interactions by producing an energetically lower lying orbital. Thus, shorter bonds may actually be weaker than longer bonds. However, the metal–ligand interactions have also contributions from M→P back-bonding and from electrostatic attraction. It is therefore difficult to predict if a

longer donor/acceptor bond is weaker or stronger than a shorter bond.

Bonding Analysis

Table 2 gives the results of the NBO analysis of the PX_3 ligands in the complexes and as free molecules. It becomes obvious that the phosphorus lone-pair orbitals have mainly s character in free PX_3 . The lone-pair orbitals acquire much more p character in the complexes where the percent s(P) contribution is clearly lower than the percent p(P) contribution.⁵¹

The atomic partial charges suggest that the PX_3 ligands are overall electron donors, because the phosphane ligands always carry a large positive charge. We want to point out that the partial charges of the PX_3 ligands show for all metals the somewhat unexpected trend $\text{PMe}_3 > \text{PF}_3 > \text{PH}_3 \gg \text{PCl}_3$. Thus, PF_3 is actually a stronger charge donor than PH_3 , while PCl_3 is clearly the weakest donor ligand. The separation of the M– PX_3 charge donation into contributions by P and by X shows that the intraligand charge exchange plays a significant

(49) Ernst, R. D.; Freeman, J. W.; Stahl, L.; Wilson, D. R.; Arif, A. M.; Nuber, B.; Ziegler, M. L. *J. Am. Chem. Soc.* **1995**, *117*, 5075–5081.

(50) Fischer, R. A.; Schulte, M. M.; Weiss, J.; Zsolnai, L.; Jacobi, A.; Huttner, G.; Frenking, G.; Boehme, C.; Vyboishchikov, S. F. *J. Am. Chem. Soc.* **1998**, *120*, 1237.

(51) The hybridization at P comes from an NBO Lewis structure of the complexes, which has no M–CO and no M– PX_3 bond. The metal atom has three lone-pair valence orbitals, and the ligands have the same Lewis structures as the free species.

Table 2. Results of the NBO Analysis at BP86/II: Hybridization of the Phosphorus Lone-Pair Orbital in the Free Ligand PX_3 and in the Complexes $(CO)_5M-PX_3$, Partial Charges q of the Phosphorus Atom and the Ligand PX_3 , Differences of the Partial Charges between the Free Ligand and the Bonded Ligand Δq , Δq_σ , and Δq_π , and Estimated $M-PX_3$ σ Charge Donation $\Delta q_\sigma(PX_3)^{a,b}$

M		PH ₃	PMe ₃	PF ₃	PCl ₃
free ligand	% s(P) lp	52.6	51.2	76.1	79.6
	% p(P) lp	47.3	48.8	23.9	20.4
	$q(P)$	-0.041	0.825	1.630	0.747
Cr	% s(P) lp	26.9	13.7	18.9	30.2
	% p(P) lp	73.1	86.3	81.1	69.8
	$q(PX_3)$	0.380	0.468	0.436	0.260
	$\Delta q(X_3)$	0.108	0.145	0.057	0.147
	$\Delta q(P)$	0.272	0.323	0.379	0.113
	$\Delta q_\pi(P)$	-0.143	-0.134	-0.141	-0.188
	$\Delta q_\sigma(P)$	0.415	0.456	0.520	0.301
	$[\Delta q_\sigma(PX_3)]^b$	0.523	0.602	0.571	0.448
Mo	% s(P) lp	33.0	24.4	37.4	22.6
	% p(P) lp	67.0	75.5	62.5	77.4
	$q(PX_3)$	0.324	0.403	0.378	0.214
	$\Delta q(X_3)$	0.110	0.145	0.051	0.124
	$\Delta q(P)$	0.214	0.258	0.327	0.090
	$\Delta q_\pi(P)$	-0.129	-0.120	-0.119	-0.175
	$\Delta q_\sigma(P)$	0.343	0.378	0.447	0.265
	$[\Delta q_\sigma(PX_3)]^b$	0.453	0.523	0.497	0.389
W	% s(P) lp	34.8	26.1	38.8	39.5
	% p(P) lp	65.2	73.9	61.0	60.5
	$q(PX_3)$	0.323	0.398	0.367	0.198
	$\Delta q(X_3)$	0.108	0.253	0.053	0.127
	$\Delta q(P)$	0.215	0.247	0.314	0.071
	$\Delta q_\pi(P)$	-0.137	-0.132	-0.140	-0.197
	$\Delta q_\sigma(P)$	0.352	0.379	0.454	0.268
	$[\Delta q_\sigma(PX_3)]^b$	0.460	0.530	0.507	0.395

^a Negative numbers indicate increases in electronic charges, positive numbers indicate decreases in electronic charges. ^b Calculated as the difference between $q(PX_3)$ and $\Delta q_\pi(P)$, assuming that the $M-PX_3$ π -charge donation is negligible.

role. The phosphorus atoms of the ligands become more positively charged in the complexes, but the trend of $\Delta q(P)$ is now $P(F_3) > P(Me_3) > P(H_3) \gg P(Cl_3)$. Thus, a significant part of the charge donation of PMe_3 and particularly of PCl_3 comes from the substituents X. Note that the charge donation $\Delta q(Cl_3)$ resulting from the chlorine atoms of PCl_3 is even *higher* than the donation of the P atom (Table 2).

The partition of the charge donation $\Delta q(P)$ in σ and π contributions shows (Table 2) that $\Delta q_\sigma(P)$ is always larger than $\Delta q_\pi(P)$; i.e., the phosphorus atom is a stronger σ donor than π acceptor. Note that the P atom of PCl_3 is clearly the weakest σ donor and the strongest π acceptor of the PX_3 ligands. However, it was shown above that the total charge donation of the PX_3 ligand is significantly larger than the charge donation of the P atom. We made an estimate of the total $M-PX_3$ σ -charge donation using the differences between $\Delta q_\pi(P)$ and $\Delta q(PX_3)$, which is based on the reasonable assumption that $M-PX_3$ π -donation is negligible. The results also given in Table 2 show that PCl_3 clearly is the weakest σ donor and the phosphorus atom of PCl_3 is the strongest π acceptor. The differences between the other PX_3 species are not very large. The ratio of σ charge donation of PX_3 and π charge acceptance of P, given by $\Delta q_\sigma(PX_3)/\Delta q_\pi(P)$, suggests the following order of ascending π -acceptor strength: $PMe_3 < PF_3 < PH_3 \ll PCl_3$. However, this trend must be regarded with some caution, because the NBO data do not say whether

Table 3. Results of the ETS Analysis at BP86/TZP^a

	Cr(CO) ₅ PH ₃ (1a)	Mo(CO) ₅ PH ₃ (2a)	W(CO) ₅ PH ₃ (3a)
ΔE_{int}	-33.65	-31.80	-36.38
ΔE_{Pauli}	81.53	70.71	83.66
ΔE_{elstat}	-64.86 (56.3) ^b	-59.44 (58.0) ^b	-71.50 (59.6) ^b
ΔE_{orb}	-50.32 (43.7) ^b	-43.07 (42.0) ^b	-48.54 (40.4) ^b
$\Delta E(A')$	-42.49	-35.69	-40.69
$\Delta E(A'')$	-7.84	-7.39	-7.86
ΔE_σ	-34.64 (68.8) ^c	-28.30 (65.7) ^c	-32.83 (67.6) ^c
ΔE_π	-15.69 (31.2) ^c	-14.78 (34.3) ^c	-15.72 (32.4) ^c
ΔE_{prep}	1.21	0.80	2.41
$\Delta E(=-D_e)$	-32.44	-31.00	-33.97
	Cr(CO) ₅ PMe ₃ (1b)	Mo(CO) ₅ PMe ₃ (2b)	W(CO) ₅ PMe ₃ (3b)
ΔE_{int}	-43.66	-40.86	-46.37
ΔE_{Pauli}	96.53	85.62	99.28
ΔE_{elstat}	-85.08 (60.7) ^b	-80.69 (63.8) ^b	-94.85 (65.1) ^b
ΔE_{orb}	-55.11 (39.3) ^b	-45.79 (36.2) ^b	-50.80 (34.9) ^b
$\Delta E(A')$	-48.03	-39.46	-44.04
$\Delta E(A'')$	-7.08	-6.33	-6.76
ΔE_σ	-40.96 (74.3) ^c	-33.13 (72.3) ^c	-37.27 (73.4) ^c
ΔE_π	-14.15 (25.7) ^c	-12.66(27.7) ^c	-13.53 (26.6) ^c
ΔE_{prep}	2.48	3.01	2.55
$\Delta E(=-D_e)$	-41.18	-37.85	-43.82
	Cr(CO) ₅ PF ₃ (1c)	Mo(CO) ₅ PF ₃ (2c)	W(CO) ₅ PF ₃ (3c)
ΔE_{int}	-35.12	-33.51	-38.56
ΔE_{Pauli}	91.96	82.28	97.00
ΔE_{elstat}	-62.85 (49.5) ^b	-57.43 (49.6) ^b	-70.16(51.8) ^b
ΔE_{orb}	-64.24 (50.5) ^b	-58.35 (50.4) ^b	-65.40 (48.2) ^b
$\Delta E(A')$	-48.45	-43.07	-48.87
$\Delta E(A'')$	-15.79	-15.29	-16.53
ΔE_σ	-32.66 (50.8) ^c	-27.77 (47.6) ^c	-32.35 (49.5) ^c
ΔE_π	-31.58 (49.2) ^c	-30.59 (52.4) ^c	-33.05 (50.5) ^c
ΔE_{prep}	1.34	2.66	3.14
$\Delta E(=-D_e)$	-33.78	-30.85	-35.42
	Cr(CO) ₅ PCl ₃ (1d)	Mo(CO) ₅ PCl ₃ (2d)	W(CO) ₅ PCl ₃ (3d)
ΔE_{int}	-27.75	-26.14	-31.05
ΔE_{Pauli}	78.40	70.14	83.29
ΔE_{elstat}	-49.56 (46.7) ^b	-45.31 (47.3) ^b	-55.82 (48.8) ^b
ΔE_{orb}	-56.59 (53.3) ^b	-50.98 (52.9) ^b	-58.51 (51.2) ^b
$\Delta E(A')$	-43.51	-38.61	-44.86
$\Delta E(A'')$	-13.08	-12.37	-13.65
ΔE_σ	-30.43 (53.7) ^c	-26.25 (51.5) ^c	-31.20 (53.3) ^c
ΔE_π	-26.16 (46.3) ^c	-24.73 (48.5) ^c	-27.31 (46.7) ^c
ΔE_{prep}	1.00	2.48	2.45
$\Delta E(=-D_e)$	-26.75	-23.66	-28.60

^a Energies are given in kcal mol⁻¹. ^b Percentage of the total attractive interactions $\Delta E_{elstat} + \Delta E_{orb}$. ^c Percentage of the total orbital interactions ΔE_{orb} .

the increase of the π charge at the P atom, $\Delta q_\pi(P)$, comes from $M \rightarrow PX_3$ π -back-donation or from intraligand charge donation $P \rightarrow X_3$ into the phosphorus $p(\pi)$ AOs. The changes in the charge distribution clearly show, however, that the PX_3 ligands are stronger σ charge donors than π charge acceptors. The ligand PCl_3 sticks out as the poorest σ donor and the strongest $\pi(P)$ acceptor. In the next section we will discuss the associated energy contributions to the $M-P$ bonds.

Table 3 presents the results of the ETS analysis of the phosphane complexes. The energy term ΔE_{prep} (eq 1) is very small, because the deformation of the fragment geometries from the equilibrium structures to the geometries in the complexes is not very large. Thus, the $M-PX_3$ interaction energies ΔE_{int} have similar values and nearly show the same trend as the D_e values. The only difference is found for the PH_3 and PF_3 complexes.

For the ΔE_{int} values of all M, the order $\text{PF}_3 > \text{PH}_3$ is observed, whereas the D_e values of the molybdenum complexes show the opposite order.

The largest contribution to the ΔE_{int} values for all complexes comes from the repulsive term ΔE_{Pauli} . The ratio of the electrostatic attraction ΔE_{elstat} to covalent attraction ΔE_{orb} shows significant differences for the different phosphanes. The larger ΔE_{elstat} than ΔE_{orb} values of the PH_3 complexes **1a–3a** suggest that the M– PH_3 bonds have more electrostatic than covalent character. The contribution of ΔE_{elstat} varies between 56.3% for the chromium complex and 59.6% for the tungsten complex. The breakdown of the orbital interaction energy into contributions from orbitals having a' and a'' symmetry gives much larger values for the former orbitals. Note that the total π -bonding energy is twice the a'' value because the M– PX_3 π -bonds are nearly degenerate.⁵⁹ The total σ and π orbital contributions to the covalent bonding are also given in Table 3. The π -bonding energy in the PH_3 complexes **1a–3a** is about one-third of ΔE_{orb} . A previous analysis of the electronic structure of **1a–3a** showed also significant contributions by covalent interactions and strong π -bonding in the metal–phosphane bonds.^{14b} We want to point out, however, that the ratio of σ and π orbital energies gives a higher π contribution than the electronic charges using the σ components $\Delta q_{\sigma}(\text{P})$ and particularly $\Delta q_{\sigma^-}(\text{PX}_3)$ together with the π components $\Delta q_{\pi}(\text{P})$ shown in Table 2.

Table 3 shows that the interaction energies ΔE_{int} of the PMe_3 complexes **1b–3b** are $\sim 10 \text{ kcal mol}^{-1}$ higher than the values of the respective PH_3 complexes **1a–3a**. All three contributions ΔE_{elstat} , ΔE_{Pauli} , and ΔE_{orb} are larger in the former species than in the latter, although the M–P bonds of **1b–3b** are longer than those of **1a–3a**. Table 2 shows that the phosphorus lone-pair donor orbital in the PMe_3 complexes has a higher percent p character than in the PH_3 complexes. This is in agreement with the energy decomposition of the orbital interaction term, demonstrating (Table 3) that the former species have a higher ΔE_{σ} contribution than the latter molecules. However, the stronger bonds of the PMe_3 complexes as compared with the PH_3 analogues are caused by the increase of the electrostatic attraction rather than by the orbital term. The ΔE_{elstat} values of **1b–3b** are $20\text{--}24 \text{ kcal mol}^{-1}$ higher than those of **1a–3a**, while the ΔE_{orb} values increase only by $2\text{--}5 \text{ kcal mol}^{-1}$. Table 3 shows that the contribution of ΔE_{elstat} of **1b–3b** varies between 60.7% for the chromium and 65.1% for the tungsten complex.

The energy decomposition analysis of the halophosphane complexes **1c–3c** and **1d–3d** reveals significant

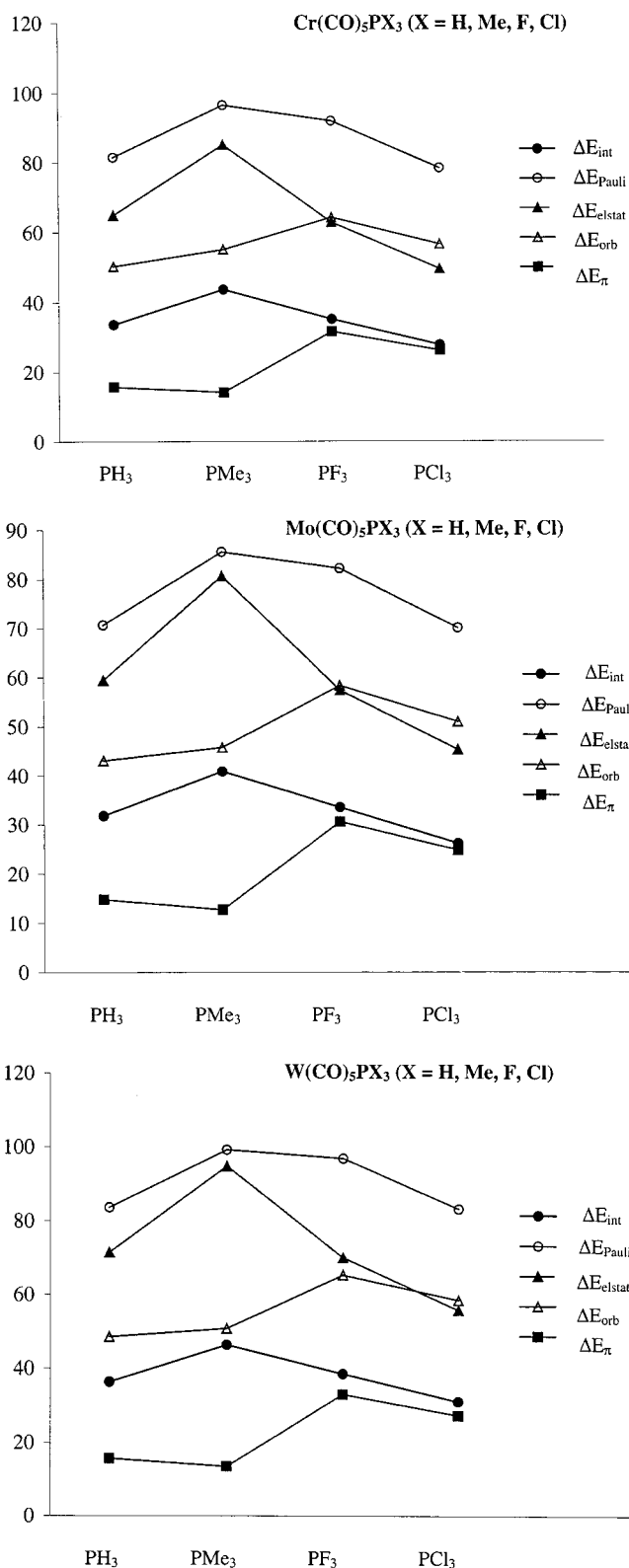


Figure 2. Correlation of the energy terms of the ETS analysis, ΔE_{elstat} , ΔE_{Pauli} , ΔE_{orb} , and ΔE_{π} , with the total interaction energy ΔE_{int} . Energy values are in kcal mol^{-1} .

differences in the PH_3 and PMe_3 complexes. Table 3 shows that the M–P bonds in the complexes with PF_3 and PCl_3 ligands have about equal electrostatic and covalent character and that the σ and π contributions to ΔE_{orb} are nearly the same. The weaker M– PCl_3 bonds have slightly less electrostatic character and smaller π contributions to ΔE_{orb} than the M– PF_3 bonds. The

(52) Lee, K. J.; Brown, T. L. *Inorg. Chem.* **1992**, *31*, 289–294.

(53) Cotton, F. A.; Darensbourg, D. J.; Kolthammer, B. W. S. *Inorg. Chem.* **1981**, *20*, 4440–4442.

(54) Bridges, D. M.; Holywell, G. C.; Rankin, D. W. H.; Freeman, J. M. *J. Organomet. Chem.* **1971**, *32*, 87–95.

(55) McRae, G. A.; Gerry, M. C. L.; Cohen, E. A. *J. Mol. Spectrosc.* **1986**, *116*, 58–70.

(56) Bryan, P. S.; Kuczowski, R. L. *J. Chem. Phys.* **1971**, *55*, 3049–3051.

(57) Morino, Y.; Kuchitsu, K.; Moritani, T. *Inorg. Chem.* **1969**, *8*, 867–871.

(58) Kisliuk, P.; Townes, C. H. *J. Chem. Phys.* **1950**, *18*, 1109–1111.

(59) The π bond of the C_{3v} symmetric M– PX_3 fragment is doubly degenerate. The two components of the π bond are slightly different in energy when the C_{3v} symmetric PX_3 ligand is bonded to the C_{4v} symmetric $M(\text{CO})_5$ fragment.

correlation between weaker bonding and less π contribution to the orbital interactions is not generally valid, however. Thus, the PMe_3 complexes **1b**–**3b** contain the strongest M–P bonds but also have the lowest π contributions to ΔE_{orb} (Table 3). This result shows that the trend in the strength of metal–ligand bonds is not determined by a single contribution alone. Figure 2 shows a correlation of the calculated energy terms with the PR_3 ligands. None of the energy contributions correlate with the trend of the total interaction energies ΔE_{int} of the phosphane ligands: $\text{PMe}_3 > \text{PF}_3 > \text{PH}_3 > \text{PCl}_3$. We want to particularly point out that neither the total orbital interaction term ΔE_{orb} nor the π contribution ΔE_{π} is in accord with the trend of the interaction energy. The best correlation is found between ΔE_{int} and ΔE_{elstat} . This result suggests that electrostatic interactions are the most important factor for the trend of the bond strength. Note, however, that the relative values of ΔE_{int} and ΔE_{elstat} of the PH_3 and PF_3 complexes do not agree.

The results shown in Table 3 suggest the order $\text{PF}_3 > \text{PCl}_3 > \text{PMe}_3 > \text{PH}_3$ for the π -bonding contributions to the M– PX_3 bonds, which is given by the absolute values of ΔE_{π} and by the relative strength given as percent ΔE_{π} . It is gratifying that the same trend was found in an energy decomposition analysis of $\text{Fe}(\text{CO})_4\text{PR}_3$ by González-Blanco and Branchadell.¹³ Their study, however, did not include the PCl_3 complex and was carried out differently with respect to the breakdown of the orbital interactions into σ and π contributions. The authors only used the frontier orbital interactions as σ and π contributions, while the remaining orbital interactions were considered as residual stabilization E_{res} . The values of E_{res} were much larger than the E_{π} values and in some cases even larger than E_{σ} .¹³ We prefer to take the sum of the σ and π contributions as a measure of E_{σ} and E_{π} , respectively.

We want to comment on the π -acceptor strength of the PCl_3 ligand, which has been suggested to be a weak π acceptor in $\text{Mo}(\text{CO})_{6-n}(\text{PCl}_3)_n$ ($n = 1-3$).²⁰ The suggestion rests on the assumption that the ⁹⁵Mo and ³¹P NMR shielding behavior of the PCl_3 ligand correlates with its π acceptor strength. A later inspection of the calculated chemical shift tensors of $\text{M}(\text{CO})_5\text{PX}_3$ ($X = \text{H, Me, Ph, F, Cl; M} = \text{Cr, Mo}$) showed, however, that PCl_3 is actually a better π acceptor than the other phosphane ligands.¹⁵ In the latter work it was suggested that the $\Delta\delta_{zz}$ components rather than the coordination shifts should be used as an indicator of back-donation. The results of the NBO analysis and particularly the energy

decomposition analysis give further evidence that PCl_3 should be classified as a strong π acceptor. The ETS analysis proves that the metal–ligand bonds of PF_3 and PCl_3 have about equal contributions from electrostatic and covalent interactions and that the σ and π contributions to the latter are of about the same strength. The M– PX_3 bonds of the ligands PH_3 and PMe_3 have less covalent character and a significantly lower degree of π bonding than PF_3 and PCl_3 .

Summary and Conclusion

The synthesis of the phosphane complexes $\text{M}(\text{CO})_5\text{PH}_3$ ($\text{M} = \text{Mo, W}$), $\text{W}(\text{CO})_5\text{PD}_3$, and $\text{W}(\text{CO})_5\text{PF}_3$ has been achieved. The X-ray diffraction analyses of $\text{W}(\text{CO})_5\text{PH}_3$ and $\text{Mo}(\text{CO})_5\text{PCl}_3$ give experimental information of important parent complexes. DFT calculations of the geometries and bond dissociation energies of $\text{M}(\text{CO})_5\text{PX}_3$ ($\text{M} = \text{Cr, Mo, W; X} = \text{H, Me, F, Cl}$) prove that there is no correlation between the bond lengths and bond energies of the M–P bonds. The BDEs of the phosphane ligands follow for all metals M the trend $\text{PMe}_3 > \text{PF}_3 \approx \text{PH}_3 > \text{PCl}_3$, while the calculated M– PX_3 interatomic distances decrease in the series $\text{PMe}_3 > \text{PH}_3 > \text{PCl}_3 > \text{PF}_3$. The energy decomposition analysis indicates that the PH_3 and PMe_3 ligands are more electrostatically than covalently bonded to the metals M. The electrostatic contribution amounts to 56–66% of the total attractive interactions $\Delta E_{\text{elstat}} + \Delta E_{\text{orb}}$. The orbital interactions in the M– PH_3 and M– PMe_3 bonds have more σ character (65–75%) than π character (25–35%). The M–P bonds of the halophosphane complexes $\text{M}(\text{CO})_5\text{PF}_3$ and $\text{M}(\text{CO})_5\text{PCl}_3$ are nearly half covalent and half electrostatic. The π bonding contributes ~50% to the total orbital interaction.

Acknowledgment. This work was supported by the Deutsche Forschungsgemeinschaft and the Fonds der Chemischen Industrie. Excellent service by the Hochschulrechenzentrum of the Philipps-Universität Marburg is gratefully acknowledged. Additional computer time was provided by the HLRS Stuttgart.

Supporting Information Available: Tables S1 and S2, giving experimental and calculated bond lengths and angle for **2d** and **3a**, Figures S1 and S2, giving experimental structures of **2d** and **3a**, and a printout of the CIF data for these two compounds. This material is available free of charge via the Internet at <http://pubs.acs.org>.

OM020311D